

Effects of Polyethylene Glycol on DNA Adsorption and Hybridization on Gold Nanoparticles and Graphene Oxide

Xu Zhang^{†‡}, Po-Jung Jimmy Huang[†], Mark R. Servos[‡] and Juewen Liu^{†*}

[†] Departments of Chemistry and Waterloo Institute for Nanotechnology, [‡] Department of Biology

University Of Waterloo, Waterloo, Ontario, N2L 3G1, Canada

Email: liujw@uwaterloo.ca

Abstract

Understanding the interface between DNA and nanomaterials is crucial for rational design and optimization of biosensors and drug delivery systems. For detection and delivery into cells, where high concentrations of cellular proteins are present, another layer of complexity is added. In this context, we employ polyethylene glycol (PEG) as a model polymer to mimic the excluded volume effect of cellular proteins and test its effect on DNA adsorption and hybridization on gold nanoparticles (AuNPs) and graphene oxide (GO), both of which show great promise for designing intracellular biosensors and drug delivery systems. We show that PEG 20,000 (e.g. 4%) accelerates DNA hybridization to DNA-functionalized AuNPs by 50-100%, but this enhanced hybridization kinetics has not been observed with free DNA. Therefore, this rate enhancement is attributed to the surface blocking effect by PEG instead of the macromolecular crowding effect. On the other hand, DNA adsorption on citrate-capped AuNP surfaces is impeded even in the presence of a trace level (i.e., parts-per-billion) of PEG, confirming PEG competes with DNA for surface binding sites. Additional insights have been obtained by studying the adsorption of a thiolated DNA and a peptide nucleic acid. In these cases, the steric effects of PEG to impede adsorption are observed. Similar observations have also been made with GO. Therefore, PEG may be used as an effective blocking agent for both hydrophilic AuNP and for GO that also contains hydrophobic domains.

This document is the Accepted Manuscript version of a Published Work that appeared in final form in Langmuir, copyright © American Chemical Society after peer review and technical editing by publisher. To access the final edited and published work see <http://dx.doi.org/10.1021/la302799s>

Introduction

Interfacing DNA with various nanomaterials has produced a diverse range of functional hybrid materials for numerous applications, including drug delivery,¹⁻³ biosensor development,⁴⁻⁹ bioelectronics,^{10,11} enzyme immobilization,^{12,13} and nanotechnology.^{14,15} DNA carries the functional roles of molecular recognition and can also act as an antisense agent.^{1,16} Gold nanoparticles (AuNPs) and graphene oxide (GO) are two representative nanomaterials for interacting with DNA. They are similar in the sense that both effectively adsorb single-stranded (ss) DNA.¹⁷⁻²¹ At the same time, both possess strong fluorescence quenching ability and good thermal and electric conductivity.^{22,23} Despite these similarities, their surface properties are quite different. AuNPs are hydrophilic while GO is planar with hydrophobic carbon-rich domains.²⁴

Two methods have been used to interface DNA with AuNPs or GO. For covalent attachment, a thiolated DNA strongly adsorbs onto AuNPs via the thiol-Au chemistry and amino-modified DNA can form an amide bond with the carboxyl on GO.^{23,25} For the other approach, ss-DNA is tightly adsorbed onto both nanomaterials,¹⁸⁻²¹ where AuNPs adsorb DNA bases via strong chemical bonding interactions while GO adsorbs DNA via aromatic stacking and hydrophobic interactions.¹⁷ Such adsorption has also been used in biosensor development,^{18-21,26-33} PCR optimization,³⁴ and materials synthesis.^{35,36}

A recent research direction is to use these hybrid materials for cellular and *in vivo* systems. For example, both mRNA and metabolites have been detected using DNA-functionalized AuNPs and GO.³⁷⁻⁴⁰ Since the environment inside a cell is very different from common buffer solutions, biosensors optimized in buffer may not work optimally in cells. While pH, temperature and ionic strength can be made to be comparable, effects caused by biomacromolecules are often neglected. For example, proteins and nucleic acids occupy 20-40% of a live cell's volume, resulting in the following two effects. First,

these biopolymers might compete for surface binding sites, thus blocking the interaction between immobilized DNA and the surface. Second, they may create a macromolecularly crowded environment, affecting the thermodynamics of reactions producing an excluded volume change such as DNA hybridization.^{41,42}

To further develop biosensors for intracellular assays, experiments need to be carried out in the presence of model polymers to simulate the cellular environment. Polyethylene glycol (PEG) is a commonly used artificial crowding agent; many biochemical reactions including protein folding and DNA melting are strongly affected by PEG.⁴²⁻⁴⁴ It needs to be pointed out that PEG is used mainly to mimic only the excluded volume effect of proteins and not their chemical properties. Most previous work on the DNA/PEG interaction has measured the melting transition of free DNA and related thermodynamic properties. We recently reported that the associated nanoparticles could further influence DNA stability. For example, PEG was able to increase the melting temperature (T_m) of DNA-functionalized AuNPs much more than that of free DNA, which was attributed to a larger excluded volume change brought by AuNPs.⁴⁵ However, the kinetic aspect of DNA hybridization and adsorption onto nanomaterials has not been systematically evaluated in the presence of PEG. Compared to thermodynamic properties, kinetic studies are more directly related to biosensor signal generation. In this work, we investigate DNA adsorption kinetics onto both unmodified and DNA-functionalized AuNPs and GO, revealing that PEG slightly increases the rate of DNA hybridization. In addition, PEG is adsorbed by unmodified AuNP and GO, impeding DNA adsorption, suggesting that PEG can be potentially used as a surface blocking agent.

Materials and Methods

Chemicals. All the DNA samples were purchased from Integrated DNA Technologies (Coralville, IA) and were purified by standard desalting. Thiolated DNA was first activated using 4×TCEP at pH 5 acetate buffer (50 mM) for 1 h. The peptide nucleic acid (PNA) sample was purchased from Biosynthesis Inc.

(Lewisville, TX) and dissolved in 0.1% trifluoroacetic acid. HAuCl_4 and tris(2carboxyethyl)phosphine (TCEP) were from Sigma-Aldrich. AuNPs (13 nm) were synthesized based on the standard citrate reduction procedures and its concentration was estimated to be ~ 10 nM.⁴⁶ Thiolated DNA (Thiol-DNA, see Table 1) functionalized AuNPs were prepared based on the established salt aging protocol.⁴⁶ All the unmodified PEG samples were purchased from VWR. FAM-labeled PEG 10,000 was purchased from Nanocs Inc. (New York, NY). GO was purchased from Advanced Chemical Suppliers (Medford, MA). Sodium citrate, sodium chloride, and 4-(2-hydroxyethyl) piperazine-1-ethanesulfonate (HEPES) were purchased from Mandel Scientific (Guelph, ON). MilliQ water was used for all experiments.

Covalent functionalization of GO with fluorescent ssDNA. The conjugation reaction was carried out for 3 h at room temperature under magnetic stirring in a glass vial with a final volume of 500 μL containing 100 $\mu\text{g}/\text{mL}$ GO, 2 μM amino-modified probe DNA (FAM-DNA- NH_2), 10 mM EDCI (freshly prepared), 25 mM NaCl and 25 mM MES (pH 6.0). The GO-DNA complex was washed extensively to remove non-covalently attached DNA as detailed in a previous publication.⁴⁷ Finally the complex was dispersed in buffer (25 mM HEPES buffer, pH 7.6, 150 mM NaCl, 1 mM MgCl_2) and stored at 4 °C with a final GO concentration of 100 $\mu\text{g}/\text{mL}$.

DNA hybridization to AuNPs and GO. DNA hybridization kinetics was studied by reacting 3'-FAM-DNA with AuNPs functionalized by Thiol-DNA. The fluorescence decay accompanying hybridization was monitored using a plate reader (Tecan Infinite F200Pro, Ex: 485 nm; Em: 535 nm). After monitoring the fluorescence of 90 μL of 10 nM 3'-FAM-DNA with a certain amount of PEG in buffer (150 mM NaCl, 20 mM HEPES, pH7.6) for 1-2 min, 10 μL of Thiol-DNA functionalized AuNPs (10 nM) were quickly added and mixed in each well, followed by kinetic monitoring. The fluorescence decay rate was fit to pseudo first order reaction model. The hybridization kinetics on GO was monitored in a similar way, where added DNA (24-mer cDNA) was not fluorescent but GO was covalently functionalized with FAM-DNA- NH_2 . Therefore, this hybridization was indicated by the increase of the

fluorescence signal because the formation of duplex DNA could position the FAM away from the GO surface. In this experiment, the 2-min baseline was first obtained by measuring the fluorescence of the GO-DNA complex (5 $\mu\text{g}/\text{mL}$ GO) dissolved in buffer (150 mM NaCl, 20 mM HEPES, pH7.6) with 2% PEG 400. Following the addition of 20 nM 24-mer cDNA, a kinetic measurement was performed.

Free DNA hybridization. The hybridization kinetics of free DNA (not associated with nanomaterials) in the presence of PEG was performed in a 100 μL volume containing 10 mM HEPES buffer (pH 7.6), 150 mM NaCl and 10 nM FAM-DNA. 20 nM Quencher-DNA was added in the absence or presence of different PEGs at room temperature. The fluorescence decrease over time was recorded by the plate reader.

DNA, thiolated DNA and PNA adsorption. The procedure of DNA and PNA adsorption experiment was similar to the hybridization experiment, except that AuNPs and GO were not functionalized with covalently attached DNA. Specifically, in the 96-well plate, the adsorption kinetics was obtained by measuring the fluorescence quenching after mixing 1 nM AuNP with 10 nM 5'FAM-DNA or FAMDNA-SH in buffer (60 mM NaCl, 5 mM HEPES, pH 7.6) containing PEGs of various MWs. Similarly, the adsorption kinetics of PNA (7 nM) onto AuNPs (1 nM) or 5'FAM-DNA (10 nM) onto GO (2 $\mu\text{g}/\text{mL}$) were monitored with the plate reader.

PEG adsorption and displacement. The FAM-labeled PEG 10,000 was dissolved in 90 μL of 5 mM HEPES buffer (pH 7.6) with a final concentration of 4 nM (0.04 ppm) for baseline measurement. Afterwards, 10 μL of 10 nM AuNPs were added with a final concentration of 1 nM to initiate the PEG adsorption with quenched fluorescence. To study displacement, the FAM-PEG 10,000/AuNP complex was purified by centrifugation and rinsed with 5 mM HEPES buffer for four times to remove the free FAM-PEG. Then 100 nM PEG with different MWs were added into each well to study the displacement of the adsorbed FAM-PEG by non-labeled PEGs.

Table 1. DNA and PNA sequences and modifications used in this work.

| Name | Sequence and modifications (from 5' to 3') |
|-------------------------|--|
| 5'FAM-DNA | FAM-CACTGACCTGGG |
| FAM-DNA-SH | FAM-ATGCGGAGGAAGGTTTT-SH |
| FAM-PNA | FAM-CACTGACCTGGG |
| Thiol-DNA | TCACAGATGCGTAAAAAAAAAA-SH |
| 3'FAM-DNA | ACGCATCTGTGA-FAM |
| FAM-DNA | TCACAGATGCGT-FAM |
| Quencher-DNA | Iowa Black FQ-ACGCATCTGTGA |
| FAM-DNA-NH ₂ | FAM-ACGCATCTGTGAAGAGAACCTGGG-NH ₂ |
| 24-mer cDNA | CCCAGGTTCTCTTCACAGATGCGT |

Results and Discussion

Effect of PEG on DNA hybridization. We first measured the DNA hybridization kinetics with DNA-functionalized AuNPs (Figure 1A). The 3'FAM-DNA (FAM=6-carboxyfluorescein, see Table 1 for DNA sequence) was respectively dissolved in buffers containing 4% (w/w) PEG with MWs ranging from 400 to 20,000 (4% PEG 400 = 100 mM; 4% PEG 20,000 = 2 mM). Hybridization was induced by adding a small volume of Thiol-DNA-functionalized AuNPs to give a final AuNP concentration of 1 nM. Since AuNPs can quench fluorescence, DNA hybridization was monitored by the decrease of fluorescence signal. The sample without PEG showed a fluorescence decay rate of 0.11 min⁻¹ (Figure 2A, black line). The hybridization kinetics was slightly faster in all tested PEGs with rates ranging from 0.14 to 0.20 min⁻¹.

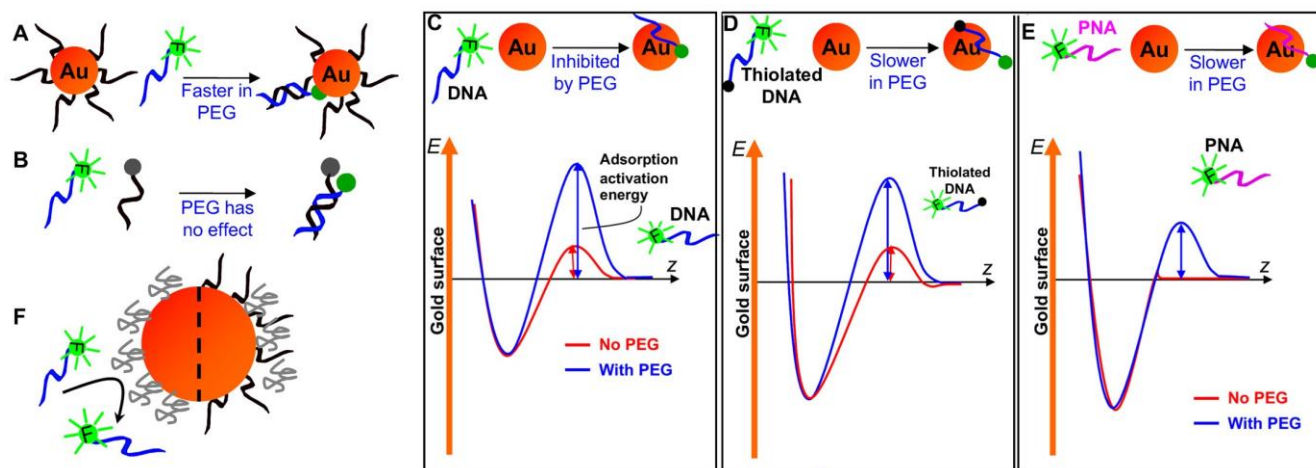


Figure 1. Schematic presentation of experiment design. (A) Hybridization of a FAM-labeled DNA with a DNA-functionalized AuNP is faster in PEG. (B) The kinetics of free DNA hybridization is not affected by PEG. Adsorption of DNA (C), thiol-modified DNA (D) and PNA (E) onto citrate-capped AuNPs is slower in PEG. In all the systems, fluorescence decreases upon adsorption. The potential energy diagrams for the adsorption reaction in the presence or absence of PEG are also shown. (F)

Schematics on the effect of PEG. The left half represents a bare AuNP with adsorbed PEG, blocking DNA adsorption. In the right half, PEG adsorption reduces the interaction between DNA and AuNP surface, leading to faster hybridization with cDNA.

For comparison, we studied free DNA hybridization using Quencher-DNA and FAM-DNA (Figure 1B). Interestingly, all the fluorescence decay curves overlapped (Figure 2B) with a decay rate of 0.63 min^{-1} , consistent with the report by Schoen *et al.* on molecular beacon hybridization in PEG.⁴⁸ Based on this observation, we reason that the macromolecular crowding effect might not be important on DNA hybridization kinetics since the excluded volume change should be similar in the presence and absence of AuNPs. Instead, we propose that PEG might block non-specific DNA/AuNP interactions and thus accelerate DNA hybridization.

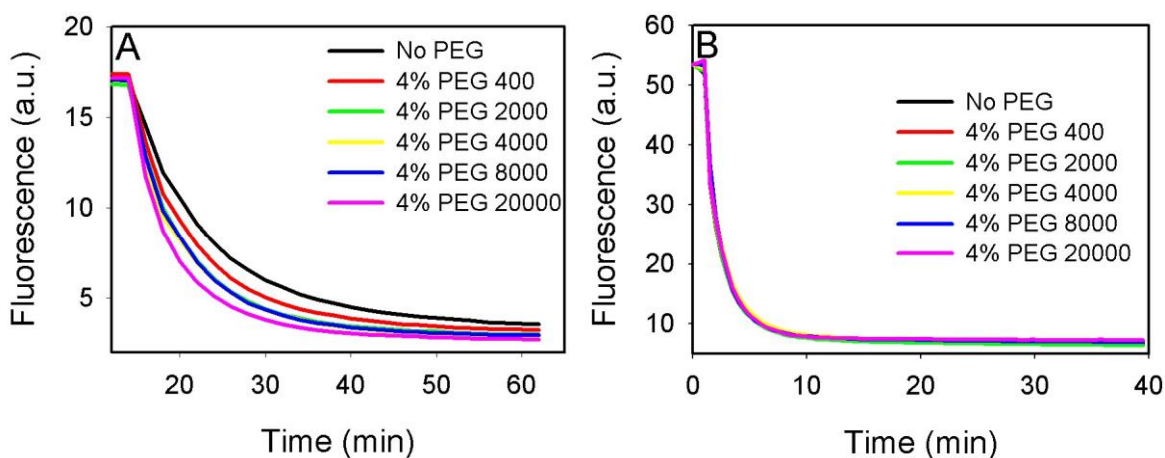


Figure 2. Kinetics of FAM-labeled DNA hybridization with DNA-functionalized AuNPs (A) or with Iowa Black FQ-labeled Quencher-DNA (B) in 4% PEG of different MWs. The buffer contained 150 mM NaCl, 5 mM HEPES, pH 7.6. AuNPs or Quencher-DNA was added after monitoring the baseline fluorescence for a few minutes.

Effect of PEG on DNA adsorption. Our AuNPs were capped by weakly adsorbed citrate that can be readily displaced by other molecules such as thiolated and even non-thiolated DNA.²¹ We and others have studied this adsorption reaction in detail and have identified the important role of salt and pH.^{21,49-51} We also reported that thiolated DNA can be attached to AuNPs in PEG⁵¹, but the effect of PEG on non-thiolated DNA adsorption has not yet been investigated. In this study, mixing 1 nM citrate-capped AuNPs with 10 nM 5'FAM-DNA resulted in an exponential decay of fluorescence with a rate of 0.94 min⁻¹ in 60 mM NaCl (Figure 3A, black curve). Higher salt concentrations were not tested to avoid AuNP aggregation. The adsorption kinetics in the presence of very dilute PEG (0.02%) was also measured. PEG 200 showed no effect on the adsorption kinetics but higher MW PEGs started to impede DNA adsorption. With PEG 1000 and above, the fluorescence barely changed in the 15 min monitored, where the initial fluorescence drop right after AuNP addition was mainly due to light extinction by AuNPs (e.g. inner filter effect). More concentrated PEG solutions (e.g. 5% PEG 20,000) also completely inhibited DNA

adsorption (data not shown). It needs to be pointed out that thiolated DNA can still be adsorbed even in the presence of PEG.⁵¹

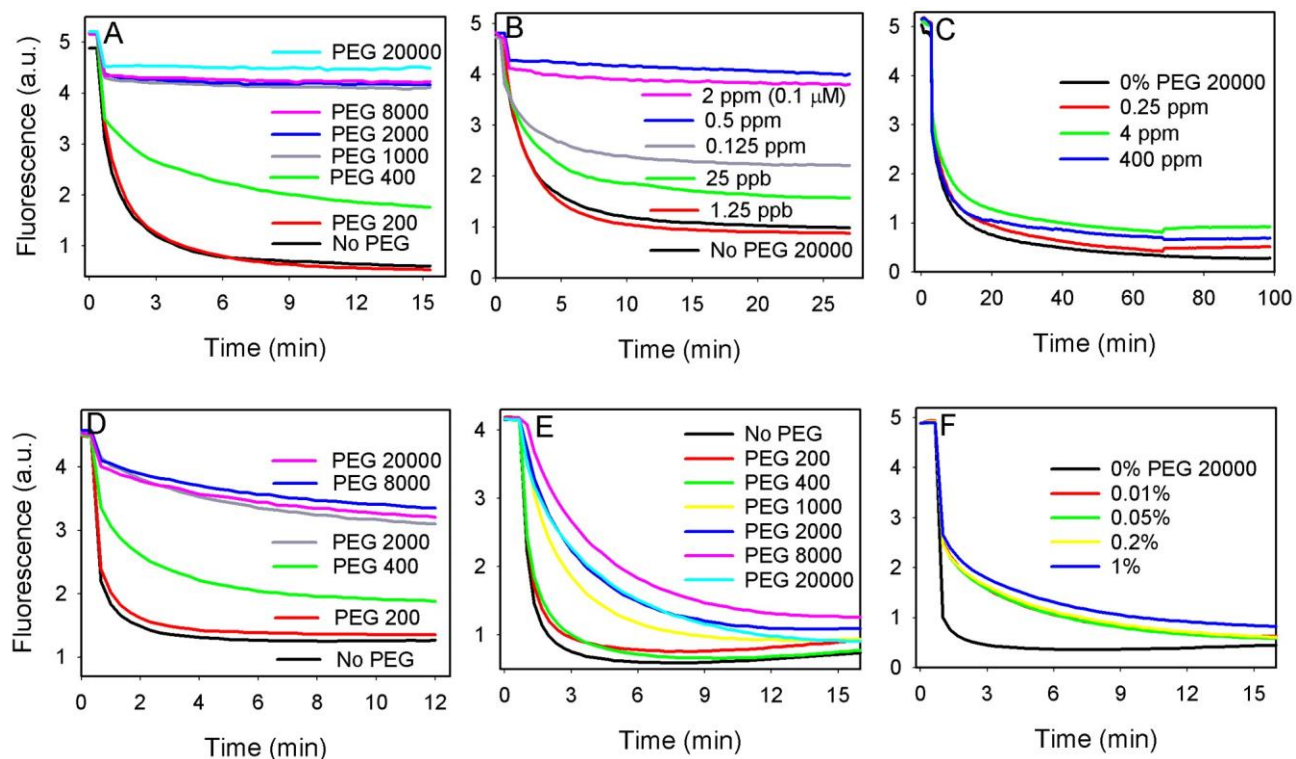


Figure 3. Adsorption onto citrate-capped AuNPs. (A) FAM-labeled DNA adsorption kinetics as a function of PEG MW (PEG concentration = 200 ppm, or 10 μ M for PEG 20,000 and 1 mM for PEG 200). PEG was mixed with AuNPs before the DNA was added. (B) Adsorption kinetics as a function of PEG 20,000 concentration. 1 ppm PEG 20,000 = 50 nM. (C) Displacement study: 5'FAM-DNA was mixed with AuNPs first and PEG 20,000 was added at the time point designated by the arrow. (D) Adsorption of FAM-DNA-SH by AuNPs with PEG 20,000 (200 ppm). FAM-labeled PNA adsorption as a function of PEG MW using 200 ppm PEG (E) and as a function of PEG 20,000 concentration (F).

This study indicates that PEG can block AuNP surface for non-thiolated DNA adsorption in a PEG MW-dependent manner. Since the experiment was carried out using the same w/w PEG concentration, the low MW PEGs had higher molar concentrations. Therefore, the stronger blocking

effect of higher MW PEGs can only be explained by their higher affinity to AuNPs. Binding between PEG and the gold surface has been proposed to be through the ether oxygen.^{52,53} Although each monomer unit might only bind weakly, a high affinity can still be achieved by polyvalent interactions. Next we tested the effect of PEG concentration (Figure 3B). With 1 nM AuNPs, the blocking effect started to occur with 25 ppb (1.25 nM) of PEG 20,000 and complete inhibition was achieved with ~0.5 ppm (25 nM). We previously measured the adsorption isotherm of FAM-labeled PEG 10,000 onto AuNPs, where comparable results were obtained.⁵¹ The hydrodynamic radius of PEG 20,000 is ~ 5 nm. Based on geometric calculation, each 13 nm AuNP can adsorb ~20 PEG 20,000 molecules. Therefore, the binding affinity between high MW PEG and AuNPs is high, approaching quantitative adsorption.

Based on the impeded and even complete inhibited DNA adsorption by high MW PEGs, we next tested whether PEG can displace adsorbed DNA. AuNPs and 5'FAM-DNA were first incubated for ~1 h and then various concentrations of PEG 20,000 were added (Figure 3C). Little change in fluorescence intensity was observed, suggesting that PEG cannot displace adsorbed DNA. Therefore, both PEG and DNA might be adsorbed with a high affinity; the displacement of either one needs to overcome a high activation energy barrier.

Effect of salt concentration. Since both DNA and AuNPs are negatively charged, DNA adsorption needs to overcome an electrostatic energy barrier that can be reduced by adding salt.⁵⁰ With adsorbed PEG, DNA adsorption needs to overcome an additional steric barrier. With large PEGs, the range of this steric barrier might overlap with the long-ranged electrostatic barrier to produce a much higher overall barrier, which may explain PEG's blocking effect. A potential energy diagram on the effect of PEG is shown in Figure 1C. With a high concentration of high MW PEG (e.g >2% PEG 20,000), a new AuNP stabilization mechanism based on depletion force arises,⁵¹ allowing AuNPs to be stably dispersed in extremely high concentration of salt. With 1 M NaCl, we obtained an adsorption capacity of 69 ± 5

5 □FAM-DNA per AuNP after 2 h incubation in the presence of 4% PEG 20,000. High salt significantly reduces electrostatic repulsion and only the steric barrier by PEG needs to be conquered.

This indicates that the adsorption affinity for DNA is higher than that for PEG since non-thiolated DNA can still chemisorb onto AuNPs via DNA bases.¹⁷

Adsorption of thiolated DNA. To gain further insights into the effect of PEG, adsorption of a thiol and FAM dual-modified DNA (FAM-DNA-SH) was tested (Figure 1D). For a fair comparison, the NaCl concentration was still 60 mM in this experiment. The adsorption kinetic traces are shown in Figure 3D, where the overall pattern was similar to that of the non-thiolated DNA. In the absence of PEG, the adsorption was the fastest (rate = $\sim 3.0 \text{ min}^{-1}$). Retarded DNA adsorption was observed in a PEG MW dependent manner, but no complete inhibition was observed. The rate of adsorption was only $\sim 0.06 \text{ min}^{-1}$ for PEG 2000 and higher, a drop of ~ 50 -fold. This experiment indicated that DNA was able to overcome both the electrostatic and steric barriers and approach the AuNP surface even with just 60 mM NaCl. Without the thiol group, however, the DNA was likely to bounce back before it could be stably adsorbed. With the thiol group, such collisions might result in stable adsorption. Therefore, thiolmodified DNA has a higher sticking coefficient. Since the electrostatic repulsion is likely to be similar in the presence or absence of PEG, this 50-fold decrease is attributed to the steric effect caused by PEG. Since the molar concentration of PEG 20,000 is ten times lower than that of PEG 2000, although the former binds more strongly, it has a lower molar concentration, leading to similar inhibition effects. The lower MW PEGs do not bind to AuNPs strongly, showing little inhibition effect. The hydrodynamic diameter of PEG 2000 is $\sim 2.5 \text{ nm}$, and electrostatic repulsion is also taking place in this region (e.g. Debye length = $\sim 1.3 \text{ nm}$ with 60 mM Na^+) so that the two barriers can overlap (Figure 1C). **PNA adsorption.** To further understand this impeded DNA adsorption, we tested a non-charged DNA analog, peptide nucleic acid (PNA) (Figure 1E). There should be no electrostatic repulsion between PNA and AuNPs. Indeed,

PNA adsorption was quite fast and fluorescence was stable after ~3 min in the absence of PEG (Figure 3E). Although PEG also impeded PNA adsorption in a MW dependent manner, the rate was still quite fast for all the samples. Next we tested the effect of PEG concentration (Figure 3F) and fast adsorption still occurred even in 1% PEG 20,000, suggesting that PNA could displace adsorbed PEG. The rate of PNA adsorption in the absence of PEG was 2.2 min^{-1} and in the presence of PEG 20,000 was 0.31 min^{-1} . This difference was only ~7 fold. For comparison, unmodified DNA was almost completely inhibited and thiolated DNA was ~50-fold slower. Therefore, the steric effect caused by PEG was more pronounced when the electrostatic barrier was high.

Based on these results, we plotted the potential energy diagram for the DNA/PNA adsorption (Figure 1C-E). For DNA adsorption, PEG creates an additional steric energy barrier that overlaps with the electrostatic barrier, leading to high adsorption activation energy. The attractive force for DNA adsorption is from DNA base chemisorption with AuNP surface,¹⁷ which is short-ranged and can take place only near the AuNP surface. In water, hydrophobic DNA bases are likely to be shielded. Even some high energy DNAs could cross the barriers, but if the DNA cannot expose its base to form a stable adsorption conformation, it will be bounced back. For thiolated DNA, although the activation energy barrier is similarly high, it has much higher adsorption energy. Once close to the surface, the chance for adsorption is higher. Finally, although the energy barrier for PNA is increased by PEG, its absolute value is still small for the lack of electrostatic contribution.

PEG adsorption and displacement. The adsorption of PEG by planar gold, platinum and other metal surfaces has been carried out using electrochemistry since PEG is a commonly used polymer additive in electrolytic baths.⁵² Our results indicate that PEG is also effectively adsorbed by AuNPs. To provide direct evidence for this adsorption we employed FAM-labeled PEG 10,000, which was indeed quickly adsorbed by AuNPs (Figure 4A). To further understand PEG adsorption, after adsorbing FAM-labeled PEG 10,000 onto AuNPs, 100 nM of non-labeled PEG was added (Figure 4B). Fluorescence increase

indicative of displacement was observed only when PEG MW was greater than 8000. Therefore, PEG adsorption is stronger with longer chains, consistent with the previous DNA adsorption experiment. PEG cannot be displaced by DNA (Figure 3C), but can be displaced by PEG, suggesting the latter displacement reaction has a lower activation energy, which is presumably due to the neutral charge property of PEG.

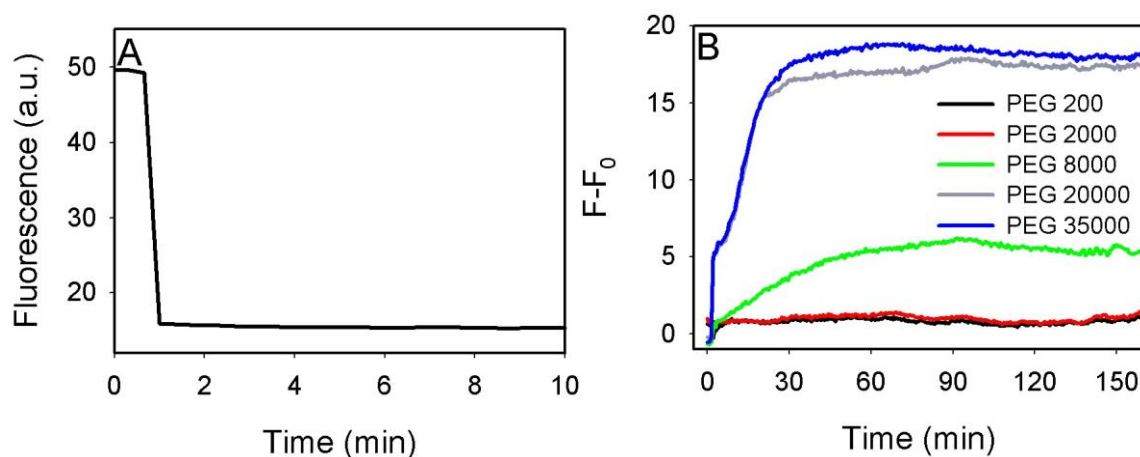


Figure 4. (A) Adsorption kinetics of FAM-labeled PEG 10,000 by AuNPs (added at 1 min). (B) Displacement of adsorbed FAM-labeled PEG 10,000 by non-labeled PEGs.

DNA adsorption onto GO. For DNA adsorption, graphene oxide (GO) shares many similar properties with AuNPs. Both have negatively charged surface, are excellent fluorescence quenchers, and selectively adsorb ss-DNA over ds-DNA.¹⁷ The major difference may be that AuNPs are hydrophilic but GO contains hydrophobic carbon domains. First, we tested the adsorption of FAM-labeled PEG 10,000 by GO (Figure 5A). The fluorescence was immediately quenched upon mixing, suggesting PEG adsorption. This adsorbed PEG can be displaced by other PEGs (Figure 5B), which is also similar to that observed for AuNPs. The kinetics of exchange was faster than that in AuNPs, suggesting that the PEG adsorption and desorption activation energy barriers might be smaller with GO than with AuNPs. Next, the effect of PEG on DNA adsorption was probed by adding 5'FAM-DNA to GO in the presence

of 1 μM PEG 8000 (Figure 5C). While PEG significantly reduced the rate of DNA adsorption, complete inhibition was not observed. Next we covalently attached amino and FAM dual-labeled DNA (FAM-DNA-NH₂) to GO using EDC as the coupling agent and monitored the hybridization kinetics with 24-mer cDNA (Figure 5D). The hybridization positioned the FAM away from the surface (but still covalently linked) to increase fluorescence. The rate of hybridization was indeed faster in the presence of PEG, similar to the case of AuNPs.

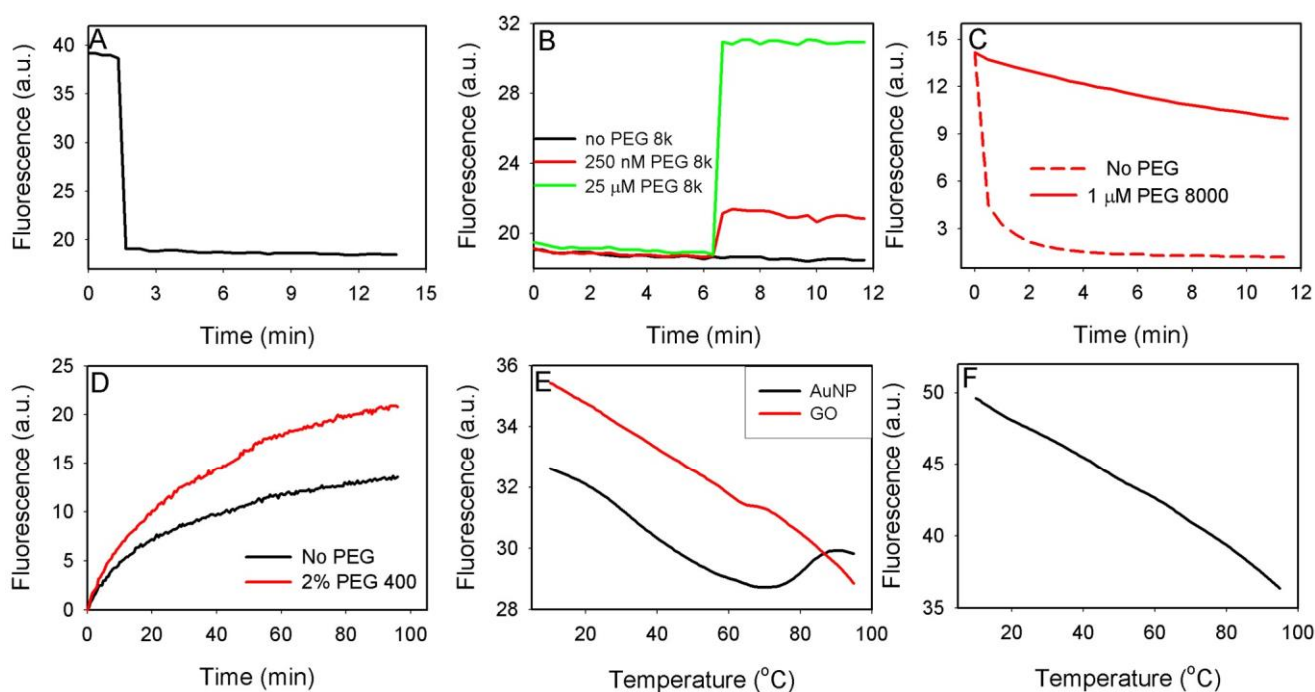


Figure 5. (A) Adsorption of FAM-labeled PEG 10,000 by GO. GO was added at 1 min. (B) Displacement of FAM-labeled PEG 10,000 by non-fluorescent PEG 8000. PEG 8000 was added at 6.5 min. (C) Adsorption of 5'FAM-DNA by GO in the presence or absence of PEG. (D) Reaction of 24mer cDNA with GO containing covalently link FAM-DNA-NH₂. (E) Fluorescence of the FAM-labeled PEG 10,000 mixed with AuNPs or GO as a function of temperature. (F) Temperature-dependent fluorescence of free FAM-labeled PEG 10,000.

Thermal desorption. To further understand PEG adsorption, we performed thermal desorption experiments. FAM-labeled PEG 10,000 was respectively adsorbed by AuNPs and GO. The samples were

then loaded into a real time PCR thermocycler and temperature-dependent fluorescence was monitored (Figure 5E). GO only showed fluorescence quenching at a rate similar to that for the free PEG (Figure 5F), indicating little desorption occurred up to 95 °C. For the PEG adsorbed on AuNPs, however, desorption was observed above 70 °C. The fact that thermal desorption did not occur on GO may suggest that PEG is adsorbed via the hydrophobic methylene groups on GO. Hydrophobic interactions are stronger at higher temperature due to the breaking of hydrogen bonds. A good example is the lower critical solution temperature (LCST) of polymer, above which polymers start to phase separate with water. The LCST is greater than 100 °C for PEG 10,000.⁵⁴ Therefore in the temperature range we tested, PEG was still fully dissolved in water. Our experiment reflects that at high temperature, PEG is more stable to be adsorbed by graphene rather than exposed to water.

Conclusions

PEG is a very useful polymer in biomedical science. It has been attached onto many nanomaterials to achieve an anti-fouling effect. Early and well-established examples include liposome and polymer nanoparticles. Recently, gold, graphene oxide, magnetic nanoparticles, quantum dots, and silica have all been capped by PEG.⁵⁵ The interaction between PEG and the surfaces are usually ignored and PEGs are pictured as a globular polymer staying on top of the particle surface. We show here that the interaction of PEG especially high MW PEGs with inorganic surfaces can be quite strong. This work has implications and applications in the following aspects. 1) Nucleic acids can be used as a probe for surface science. We first noticed the effect of PEG adsorption by AuNPs when performing the DNA adsorption experiment. To fully understand this observation, we tested thiol-modified DNA and PNA to compare the effect of adsorption strength and charge. With the advanced DNA synthesis technology, the property of DNA can be precisely controlled so that they can interact with various surfaces. In this regard, DNA was used as a probe to understand surface science. 2) Implications for drug delivery. Currently, DNA-functionalized

nanomaterials have emerged as a new platform for drug delivery, and the role of DNA ranges from a targeting ligand (e.g. cancer targeting aptamer), a detection probe (e.g. signaling aptamers and mRNA probes), to an antisense agent. To increase the *in vivo* circulation time, PEG is often added. Our study suggests that due to a lack of electrostatic repulsion thiolated PEG is likely to adsorb faster than thiolated DNA if they mix with AuNPs together. To achieve good control on the ratio between PEG and DNA, their ratio and the order of addition need to be carefully adjusted. 3) For analytical applications, since PEG can bind to both hydrophilic and hydrophobic surfaces, it can be used as a cost-effective and chemically inert blocking agent. DNA surface hybridization was slightly faster on both AuNP and GO surfaces. Compared to bovine serum albumin (BSA), a commonly used blocking agent, the property of PEG can be easily controlled by adjusting its MW. Most previous use of PEG as a blocking agent involves covalent PEG attachment. We show that adding PEG in a way similar to BSA could also be effective in blocking non-specific DNA binding interactions. Figure 1F summarizes the effect of PEG on DNA adsorption and hybridization. 4) DNA hybridization inside a cell. One of the main motivations of the work is to understand DNA hybridization kinetics in cellular environment, where concentrated proteins and nucleic acids create a crowding environment. Our work showed that using PEG as a model polymer, the free DNA hybridization kinetics was not affected. Moderate acceleration was observed for DNA probes attached to AuNPs and GO, which was attributed to the blocking effect of PEG to reduce non-specific probe/surface interactions. We can conclude that the macromolecular crowding effect alone does not contribute much to DNA hybridization kinetics.

Acknowledgements

Funding for this work is from the University of Waterloo, the Canadian Foundation for Innovation, Ontario Ministry of Research & Innovation, the Ontario Early Researcher Award, Canadian Institutes of Health Research, and the Discovery Grant of the Natural Sciences and Engineering Research Council (NSERC) of Canada.

References:

- (1) Giljohann, D. A.; Seferos, D. S.; Daniel, W. L.; Massich, M. D.; Patel, P. C.; Mirkin, C. A. Gold Nanoparticles for Biology and Medicine. *Angew. Chem. Int. Ed.* **2010**, *49*, 3280-3294.
- (2) Farokhzad, O. C.; Jon, S. Y.; Khademhosseini, A.; Tran, T. N. T.; LaVan, D. A.; Langer, R. Nanoparticle-Aptamer Bioconjugates: A New Approach for Targeting Prostate Cancer Cells. *Cancer Res.* **2004**, *64*, 7668-7672.
- (3) Allen, T. M.; Cullis, P. R. Drug Delivery Systems: Entering the Mainstream. *Science* **2004**, *303*, 1818-1822.
- (4) Rosi, N. L.; Mirkin, C. A. Nanostructures in Biodiagnostics. *Chem. Rev.* **2005**, *105*, 1547-1562.
- (5) Liu, J.; Cao, Z.; Lu, Y. Functional Nucleic Acid Sensors. *Chem. Rev.* **2009**, *109*, 1948-1998.
- (6) Wang, H.; Yang, R. H.; Yang, L.; Tan, W. H. Nucleic Acid Conjugated Nanomaterials for Enhanced Molecular Recognition. *ACS Nano* **2009**, *3*, 2451-2460.
- (7) Li, D.; Song, S. P.; Fan, C. H. Target-Responsive Structural Switching for Nucleic Acid-Based Sensors. *Acc. Chem. Res.* **2010**, *43*, 631-641.
- (8) Navani, N. K.; Li, Y. Nucleic Acid Aptamers and Enzymes as Sensors. *Curr. Opin. Chem. Biol.* **2006**, *10*, 272-281.
- (9) Zhao, W.; Brook, M. A.; Li, Y. Design of Gold Nanoparticle-Based Colorimetric Biosensing Assays. *ChemBioChem* **2008**, *9*, 2363-2371.
- (10) Xiao, Y.; Patolsky, F.; Katz, E.; Hainfeld, J. F.; Willner, I. "Plugging into Enzymes": Nanowiring of Redox Enzymes by a Gold Nanoparticle. *Science* **2003**, *299*, 1877-1881.
- (11) Zhou, M.; Dong, S. Bioelectrochemical Interface Engineering: Toward the Fabrication of Electrochemical Biosensors, Biofuel Cells, and Self-Powered Logic Biosensors. *Acc. Chem. Res.* **2011**, *44*, 1232-1243.

- (12) Kim, J.; Grate, J. W.; Wang, P. Nanostructures for Enzyme Stabilization. *Chem. Eng. Sci.* **2006**, *61*, 1017-1026.
- (13) Yoshimoto, K.; Nishio, M.; Sugasawa, H.; Nagasaki, Y. Direct Observation of Adsorption-Induced Inactivation of Antibody Fragments Surrounded by Mixed-PEG Layer on a Gold Surface. *J. Am. Chem. Soc.* **2010**, *132*, 7982-7989.
- (14) Storhoff, J. J.; Mirkin, C. A. Programmed Materials Synthesis with DNA. *Chem. Rev.* **1999**, *99*, 1849-1862.
- (15) Katz, E.; Willner, I. Nanobiotechnology: Integrated Nanoparticle-Biomolecule Hybrid Systems: Synthesis, Properties, and Applications. *Angew. Chem., Int. Ed.* **2004**, *43*, 6042-6108.
- (16) Cutler, J. I.; Auyeung, E.; Mirkin, C. A. Spherical Nucleic Acids. *J. Am. Chem. Soc.* **2012**, *134*, 1376-1391.
- (17) Liu, J. Adsorption of DNA onto Gold Nanoparticles and Graphene Oxide: Surface Science and Applications. *Phys. Chem. Chem. Phys.* **2012**, *14*, 10485-10496.
- (18) Lu, C. H.; Yang, H. H.; Zhu, C. L.; Chen, X.; Chen, G. N. A Graphene Platform for Sensing Biomolecules. *Angew. Chem. Int. Ed.* **2009**, *48*, 4785-4787.
- (19) He, S. J.; Song, B.; Li, D.; Zhu, C. F.; Qi, W. P.; Wen, Y. Q.; Wang, L. H.; Song, S. P.; Fang, H. P.; Fan, C. H. A Graphene Nanoprobe for Rapid, Sensitive, and Multicolor Fluorescent DNA Analysis. *Adv. Funct. Mater.* **2010**, *20*, 453-459.
- (20) Wu, M.; Kempaiah, R.; Huang, P.-J. J.; Maheshwari, V.; Liu, J. Adsorption and Desorption of DNA on Graphene Oxide Studied by Fluorescently Labeled Oligonucleotides. *Langmuir* **2011**, *27*, 2731-2738.
- (21) Li, H.; Rothberg, L. J. Label-Free Colorimetric Detection of Specific Sequences in Genomic DNA Amplified by the Polymerase Chain Reaction. *J. Am. Chem. Soc.* **2004**, *126*, 10958-10961.

- (22) Dubertret, B.; Calame, M.; Libchaber, A. J. Single-Mismatch Detection Using Gold-Quenched Fluorescent Oligonucleotides. *Nat. Biotechnol.* **2001**, *19*, 365-370.
- (23) Huang, P.-J. J.; Liu, J. DNA-Length-Dependent Fluorescence Signaling on Graphene Oxide Surface. *Small* **2012**, *8*, 977-983.
- (24) Gomez-Navarro, C.; Meyer, J. C.; Sundaram, R. S.; Chuvilin, A.; Kurasch, S.; Burghard, M.; Kern, K.; Kaiser, U. Atomic Structure of Reduced Graphene Oxide. *Nano Lett.* **2010**, *10*, 1144-1148.
- (25) Mirkin, C. A.; Letsinger, R. L.; Mucic, R. C.; Storhoff, J. J. A DNA-Based Method for Rationally Assembling Nanoparticles into Macroscopic Materials. *Nature* **1996**, *382*, 607-609.
- (26) Zhang, J.; Wang, L. H.; Pan, D.; Song, S. P.; Boey, F. Y. C.; Zhang, H.; Fan, C. H. Visual Cocaine Detection with Gold Nanoparticles and Rationally Engineered Aptamer Structures. *Small* **2008**, *4*, 1196-1200.
- (27) Lee, J. H.; Wang, Z.; Liu, J.; Lu, Y. Highly Sensitive and Selective Colorimetric Sensors for Uranyl (UO_2^{2+}): Development and Comparison of Labeled and Label-Free DNazyme-Gold Nanoparticle Systems. *J. Am. Chem. Soc.* **2008**, *130*, 14217-14226.
- (28) Wang, W.; Chen, C.; Qian, M.; Zhao, X. S. Aptamer Biosensor for Protein Detection Using Gold Nanoparticles. *Anal. Biochem.* **2008**, *373*, 213-219.
- (29) Wang, Z.; Lee, J. H.; Lu, Y. Label-Free Colorimetric Detection of Lead Ions with a Nanomolar Detection Limit and Tunable Dynamic Range by Using Gold Nanoparticles and Dnazyme. *Adv. Mater.* **2008**, *20*, 3263-3267.
- (30) Wei, H.; Li, B.; Li, J.; Dong, S.; Wang, E. Dnazyme-Based Colorimetric Sensing of Lead (Pb^{2+}) Using Unmodified Gold Nanoparticle Probes. *Nanotechnology* **2008**, *19*, 095501.
- (31) Wang, L.; Liu, X.; Hu, X.; Song, S.; Fan, C. Unmodified Gold Nanoparticles as a Colorimetric Probe for Potassium DNA Aptamers. *Chem. Comm.* **2006**, 3780-3782.

- (32) Wang, J.; Wang, L. H.; Liu, X. F.; Liang, Z. Q.; Song, S. P.; Li, W. X.; Li, G. X.; Fan, C. H. A Gold Nanoparticle-Based Aptamer Target Binding Readout for Atp Assay. *Adv. Mater.* **2007**, *19*, 39433946.
- (33) Zheng, X.; Liu, Q.; Jing, C.; Li, Y.; Li, D.; Luo, W.; Wen, Y.; He, Y.; Huang, Q.; Long, Y.-T.; Fan, C. Catalytic Gold Nanoparticles for Nanoplasmonic Detection of DNA Hybridization. *Angew. Chem., Int. Ed.* **2011**, *50*, 11994-11998.
- (34) Li, H. K.; Huang, J. H.; Lv, J. H.; An, H. J.; Zhang, X. D.; Zhang, Z. Z.; Fan, C. H.; Hu, J. Nanoparticle PCR: Nanogold-Assisted PCR with Enhanced Specificity. *Angew. Chem. Int. Ed.* **2005**, *44*, 5100-5103.
- (35) Wang, Z.; Zhang, J.; Ekman, J. M.; Kenis, P. J. A.; Lu, Y. DNA-Mediated Control of Metal Nanoparticle Shape: One-Pot Synthesis and Cellular Uptake of Highly Stable and Functional Gold Nanoflowers. *Nano Lett.* **2010**, *10*, 1886-1891.
- (36) Xu, L.; Zhu, Y.; Ma, W.; Chen, W.; Liu, L.; Kuang, H.; Wang, L.; Xu, C. New Synthesis Strategy for DNA Functional Gold Nanoparticles. *J. Phys. Chem. C* **2011**, *115*, 3243-3249.
- (37) Seferos, D. S.; Giljohann, D. A.; Hill, H. D.; Prigodich, A. E.; Mirkin, C. A. Nano-Flares: Probes for Transfection and Mrna Detection in Living Cells. *J. Am. Chem. Soc.* **2007**, *129*, 1547715479.
- (38) Zheng, D.; Seferos, D. S.; Giljohann, D. A.; Patel, P. C.; Mirkin, C. A. Aptamer Nano-Flares for Molecular Detection in Living Cells. *Nano Lett.* **2009**, *9*, 3258-3261.
- (39) Wang, Y.; Li, Z. H.; Hu, D. H.; Lin, C. T.; Li, J. H.; Lin, Y. H. Aptamer/Graphene Oxide Nanocomplex for in Situ Molecular Probing in Living Cells. *J. Am. Chem. Soc.* **2010**, *132*, 9274-9276.
- (40) Liu, Z.; Robinson, J. T.; Sun, X. M.; Dai, H. J. PEGylated Nanographene Oxide for Delivery of Water-Insoluble Cancer Drugs. *J. Am. Chem. Soc.* **2008**, *130*, 10876-10877.
- (41) Zhou, H.-X.; Rivas, G.; Minton, A. P. Macromolecular Crowding and Confinement: Biochemical, Biophysical, and Potential Physiological Consequences. *Ann. Rev. Biophys.* **2008**, *37*, 375-397.

- (42) Miyoshi, D.; Sugimoto, N. Molecular Crowding Effects on Structure and Stability of DNA. *Biochimie* **2008**, *90*, 1040-1051.
- (43) Miyoshi, D.; Karimata, H.; Sugimoto, N. Hydration Regulates Thermodynamics of GQuadruplex Formation under Molecular Crowding Conditions. *J. Am. Chem. Soc.* **2006**, *128*, 7957-7963.
- (44) Goodrich, G. P.; Helfrich, M. R.; Overberg, J. J.; Keating, C. D. Effect of Macromolecular Crowding on DNA: Au Nanoparticle Bioconjugate Assembly. *Langmuir* **2004**, *20*, 10246-10251.
- (45) Zaki, A.; Dave, N.; Liu, J. Amplifying the Macromolecular Crowding Effect Using Nanoparticles. *J. Am. Chem. Soc.* **2012**, *134*, 35-38.
- (46) Storhoff, J. J.; Elghanian, R.; Mucic, R. C.; Mirkin, C. A.; Letsinger, R. L. One-Pot Colorimetric Differentiation of Polynucleotides with Single Base Imperfections Using Gold Nanoparticle Probes. *J. Am. Chem. Soc.* **1998**, *120*, 1959-1964.
- (47) Huang, P.-J. J.; Liu, J. A Molecular Beacon Lighting up on Graphene Oxide. *Anal. Chem.* **2012**.
- (48) Schoen, I.; Krammer, H.; Braun, D. Hybridization Kinetics Is Different inside Cells. *Proc. Natl. Acad. Sci. U.S.A.* **2009**, *106*, 21649-21654.
- (49) Nelson, E. M.; Rothberg, L. J. Kinetics and Mechanism of Single-Stranded DNA Adsorption onto Citrate-Stabilized Gold Nanoparticles in Colloidal Solution. *Langmuir* **2011**, *27*, 1770-1777.
- (50) Zhang, X.; Servos, M. R.; Liu, J. Surface Science of DNA Adsorption onto Citrate-Capped Gold Nanoparticles. *Langmuir* **2012**, *28*, 3896-3902.
- (51) Zhang, X.; Servos, M. R.; Liu, J. Ultrahigh Nanoparticle Stability against Salt, PH and Solvent with Retained Surface Accessibility via Depletion Stabilization. *J. Am. Chem. Soc.* **2012**, *134*, 9910-9913.
- (52) Mendez, A.; Moron, L. E.; Ortiz-Frade, L.; Meas, Y.; Ortega-Borges, R.; Trejo, G. Thermodynamic Studies of PEG (MW 20,000) Adsorption onto a Polycrystalline Gold Electrode. *J. Electrochem. Soc.* **2011**, *158*, F45-F51.
- (53) Kim, J.-W.; Lee, J.-Y.; Park, S.-M. Effects of Organic Additives on Zinc Electrodeposition at

Iron Electrodes Studied by EQCM and in situ STM. *Langmuir* **2003**, *20*, 459-466.

(54) Saeki, S.; Kuwahara, N.; Nakata, M.; Kaneko, M. Upper and Lower Critical Solution

Temperatures in Poly (Ethylene Glycol) Solutions. *Polymer* **1976**, *17*, 685-689.

(55) Karakoti, A. S.; Das, S.; Thevuthasan, S.; Seal, S. Pegylated Inorganic Nanoparticles. *Angew.*

Chem. Int. Ed. **2011**, *50*, 1980-1994.